Molecular Biotechnology
https://doi.org/10.1007/s12033-024-01050-8

ORIGINAL PAPER

Hyperbaric Oxygen Upregulates Mst1 to Activate Keap1/Nrf2/HO-1 Pathway Resisting Oxidative Stress in a Rat Model of Acute Myocardial Infarction

Jianhui Liu[1] · Yan Li[1] · Shubiao Wu[2] · Zhigang Zhang[1] · Di Li[1]

Received: 1 August 2023 / Accepted: 27 December 2023

Abstract

This study aimed to investigate the protective effects and mechanisms of hyperbaric oxygen (HBO) preconditioning in a rat model of acute myocardial infarction (MI) established by ligation of the left anterior descending (LAD) coronary artery. Microarray, real-time PCR, and western blotting (WB) results demonstrated that the *Mst1* gene was downregulated in the heart tissue of the MI rat model. HBO preconditioning significantly increased Mst1 expression in cardiac tissues of rats after MI modeling. Lentiviral infection was used to silence the *Mst1* gene in rats treated with HBO to probe the effect of Mst1 on HBO cardioprotection. HBO preconditioning decreased heart infarct size and ameliorated cardiac function in MI rats, whereas *Mst1* silencing reversed the effect of HBO administration, as indicated after heat infarct size determination via TTC staining, histological examination via HE staining, and measurements of cardiac function. HBO preconditioning reduced oxidative stress and inflammation in cardiac tissue of MI rat model, evidenced by alteration of malondialdehyde (MDA), 8-hydroxy-2-deoxyguanosine (8-OHdG), and protein carbonyl contents, as well as production of inflammation-associated myeloperoxidase (MPO), IL-1β, and TNF-α. These findings provide a new signaling mechanism through which HBO preconditioning can protect against acute MI injury through the Mst1-mediating Keap1/Nrf2/HO-1-dependent antioxidant defense system.

Keywords Hyperbaric oxygen · Myocardial infarction · Mst1 · Cardiac function · Myocardial infarct

Introduction

Mortality and morbidity worldwide are mainly caused by acute myocardial infarction (MI) and subsequent heart failure. Myocardial blood flow loss due to coronary artery occlusion leads to cardiac myocyte death and myocardial remodeling. Cardiac remodeling following acute MI decreases left ventricular contraction, which consequently causes heart failure [1]. Enhanced myocardial neovascularization after acute MI may ameliorate cardiac function and decrease heart failure, and the underlying therapeutic angiogenesis represents a critical treatment scheme in post-MI treatment.

Hyperbaric oxygen (HBO) treatment can dramatically reduce the oxygen concentration in hypoperfused tissues, and elevated oxygen concentration in hypoxic tissues facilitates ischemic recovery [2, 3]. Enhanced neovascularization in ischemic tissue is one of the ways HBO therapy promotes wound healing [4]. HBO was capable of protecting hearts via anti-apoptotic effects and reducing infarct size [5, 6]. Also, the results of some clinical trials have confirmed that

✉ Di Li
lidi395@126.com

Jianhui Liu
15631073629@163.com

Yan Li
liyan950000@163.com

Shubiao Wu
hdsgyyzkzx@126.com

Zhigang Zhang
13582602449@163.com

[1] Emergency Department, Affiliated Hospital of Hebei Engineering University, Congtai District, No. 81, Congtai Road, Handan 056008, Hebei, China

[2] Department of Orthopaedics, Affiliated Hospital of Hebei Engineering University, Handan 056008, Hebei, China

Published online: 23 February 2024

HBO is advantageous for patients with acute coronary syndrome by decreasing infarct size and the incidence of severe cardiovascular cases [7]. HBO treatment results in decreased oxidative stress, anti-inflammation, cholinergic nerve protection, and neuronal apoptosis delay [8, 9]. HBO treatment can also shield PC12 cells from impairment resulting from oxygen–glucose deprivation/reperfusion [10].

Mst1 is a serine threonine kinase and a constituent of the "Hippo" pathway and has been explored during various reperfusion impairments that occur during organ transplantation [11]. As a pivotal regulator of oxidative stress, Mst1 is strongly correlated with autophagic activity and mitochondrial function. Nrf2 serves as an oxidative stress sensor and a pivotal transcription factor that can shield cells against oxidative impairment [12] and is capable of binding to its inhibitor Keap1. Once cells undergo excessive oxidative stress, Nrf2 is released from Keap1 and transferred to the nucleus, in which Nrf2 accumulates. Nrf2 binds to genes encoding antioxidant response elements (ARE), which can alleviate oxidative impairment and maintain cellular redox homeostasis. Thus, a series of genes can be transcriptionally activated, which encode cytoprotection, anti-oxidation, and anti-inflammatory proteins [13], thereby decreasing oxidative stress impairment. Nrf2 protects against oxidative stress and inflammation during retinal ischemia–reperfusion (IR) impairment [14]. Keap1/Keap1/HO-1 system is considered the main cellular defense mechanism against xenobiotics and oxidative stress [15]. A previous study displayed the protection of Mst1 against cardiac IR impairment by activating the Keap1/Nrf2 axis and repressing reactive oxygen species (ROS) production.

The relationship between HBO treatment and the Mst1-associated Keap1/Nrf2/HO-1 pathway in acute MI remains unclear. This study aimed to probe the detailed mechanism of HBO preconditioning via the Keap1/Nrf2/HO-1 pathway in MI animals. MI modeling induced decreased Mst1 expression and deactivated the Keap1/Nrf2/HO-1 pathway. However, HBO preconditioning upregulated Mst1 expression. Then, *Mst1* was silenced in vivo in HBO-preconditioned MI rats to elucidate its underlying molecular mechanism and evaluate the participation of Mst1 during the HBO-alleviated pathological process of IR injury.

Materials and Methods

Acute MI Model Establishment

An acute MI rat model was established by ligating the left anterior descending (LAD) coronary artery [16]. Wistar rats (male, 280–330 g) were used in this study. The study was approved by the ethics committee of Affiliated Hospital of Hebei Engineering University, as per the Chinese Guidance of Humane Laboratory Animal Use guidelines [Approval number: (Beijing Ammerseth Biotechnology Co., LTD, 2021078XYZ02)]. After anesthesia with isoflurane (2%) and confirmation of a totally anesthetized state (did not respond to toe pinching), the rats were placed on a rodent respirator for tracheotomy. The hearts were quickly exteriorized, and a 6-0 silk suture was tightened around the LAD proximal coronary artery (prior to the first diagonal artery branch). Control rats underwent similar procedures, except for LAD ligation. After the surgery, the wound was closed to restore normal respiration. In the acute MI study, rats were arbitrarily classified into five groups: (1) control, (2) MI alone, (3) MI and HBO pretreatment, (4) MI modeling, HBO treatment, and lentiviral (LV)-siRNA negative control (siNC) treatment, and (5) MI modeling, HBO treatment, and LV-siRNA Mst1 (siMst) treatment. After 1 h, the viable myocardium bordering the left ventricular infarct region was injected with 100 µL lentiviruses (1000 U) at three different areas.

HBO Preconditioning

In the HBO-PC group, rats were pretreated with four daily HBO (2.0 atmosphere absolute, ATA), rested for 1 day, and then were subjected to myocardial I/R surgery.

During HBO treatment, rats were confined to a hyperbaric chamber. The oxygen (100%) flow rate was set at 2.5 L/min to maintain the RT. Rats in the MI + HBO group were exposed to HBO at 2 ATA once daily for 1 h during different time periods. The oxygen pressure was selected using human treatment protocols as a reference [17]. Control rats were exposed to normobaric air at 1.0 ATA.

Finally, rats were anesthetized and sacrificed through isoflurane overdose, and their hearts were rapidly removed and kept in liquid N_2. Left ventricular tissue was subjected to western blotting (WB) and immunofluorescence staining. The infarct size was determined using the TTC method and calculated using computerized morphometry. All procedures were approved by the Animal Care and Use Committee of Affiliated Hospital of Hebei Engineering University.

Infarct Size Measurement

After reperfusion for 2 h, the suture was removed prior to infusion of 2% Evans blue dye into the aortic root to mark the area at risk (AAR, blue dye negative). TTC staining was used to measure infarct size. Briefly, hearts were harvested and stored at 20 °C for 0.5 h. Subsequently, frozen hearts were sliced into 1-mm sections parallel to the atrioventricular groove, which were thawed and incubated using 1% TTC PBS (pH 7.4) for 15 min at 37 °C. Next, they were washed with PBS and subjected to 10% formalin fixation to increase the contrast between TTC and Evans blue staining. Then, the sections were placed on a light table, and photos were taken

on both sides. Different regions were delineated. Infarct size was expressed as [white area (infarct area volume)/nonblue area (AAR)]%.

H&E Staining

Here, after collection and washing with normal saline, hearts were subjected to 4% formaldehyde fixation for 2 days and paraffin embedding; then, they were sliced into 4-mm-thick serial sections. Butterfly-shaped sections were cut and subjected to histopathological analysis. Briefly, sections were subjected to xylene deparaffinization and absolute alcohol rehydration. After rinsing with distilled water, the cells were stained with hematoxylin for 8 min. Subsequently, the sections were rinsed for 5 min under running tap water and differentiated for 0.5 min using 1% acid alcohol. After rinsing with tap water and saturated Li_2CO_3 solution, the sections were washed with 95% alcohol and subjected to eosin–phloxine counterstaining. Finally, the sections were exposed to alcohol dehydration and xylene-based mounting medium, and subsequently evaluated for cardiomyocyte hydropic alterations, neutrophilic and lymphohistiocytic infiltrates, hemorrhage, and acute myocardial necrosis.

Cardiac Function Assessment

Cardiac function was determined as described in a previous study [18]. Rats were administered chloral hydrate (300 mg/kg) as anesthesia, 24 days after I/R treatment. A small incision was made in the right midline of the neck. A microtip pressure-transducer catheter was introduced into the external right carotid artery. The proximal end of the catheter is linked to an electrostatic chart recorder. After the arterial blood pressure was detected, the catheter tip was inserted deeper until it reached the left ventricular lumen. The left ventricular pressure (LVP) signal was constantly observed and used to calculate the left ventricular systolic pressure (LVSP), developed pressure (LVDP), and $\pm(dP/dt)$ max.

MDA, GSH Activity, and 8-OHdG Measurement in Myocardium Tissues

Myocardial tissues were homogenized in 2 mL phosphate buffer (pH 7.4, 10 mM). After centrifugation for 0.5 h at $10{,}000 \times g$, the malondialdehyde (MDA), GSH, and 8-hydroxy-2-deoxyguanosine (8-OHdG) contents in the supernatant were determined. A BCA assay kit was used to measure protein concentrations.

Inflammation Determination

Cardiac tissues were collected, rinsed with normal saline, and homogenized in saline (25 mg/mL) on ice. Myeloperoxidase (MPO), IL-1β, IL-6, and IFN-α levels in cardiac tissues and cells were determined using ELISA kits (Sigma, St. Louis, Missouri) as per relevant guidelines.

Real-Time PCR

Total RNA was extracted from cardiac tissue or cardiomyocytes using TRIzol®. cDNA was obtained through the reverse transcription of RNA at 42 °C for 1 h and at 75 °C for 5 min. qPCR was performed using a SYBR Green PCR Master Kit. The thermocycling conditions were the following: first denaturation at 95 °C for 3 min; 40 cycles at 95 °C for 0.5 min, 56 °C for 0.5 min, and 72 °C for 0.5 min. The fold alteration in gene expression was obtained using the $2^{-\Delta\Delta Cq}$ method [19]. The sequences of primers used in this experiment are listed as follows: Mst1 F, 5′-CCT TGG TGC TTC ACA TCT CGA C-3′; Mst1 R, 5′-GAG CCA CGA TAC TGT TCA CCT G-3′; GAPDH F, 5′-GCA CCG TCA AGG CTG AGA A-3′; GAPDH R, 5′-TGG TGA AGA CGC CAG TGG A-3′. mRNA expression was normalized to that of GAPDH. All experiments were conducted in triplicate.

Western Blotting (WB)

The proteins from heart tissue and cells were extracted using RIPA lysis buffer according to the relevant protocol. The total protein concentration was measured. The loaded protein samples were subjected to SDS-PAGE and then transferred to Hybond-C membranes, which were incubated overnight with the appropriate primary antibodies. Bound antibodies were subsequently observed using secondary antibodies conjugated to HRP. The information of primary antibody was listed here: anti-Mst1 antibody (1:1000, ab76822, Abcam), anti-Actin (1:5000, 1:5000, ab8227, Abcam), anti-IL-1beta (1:1000, ab9722, Abcam), anti-TNF-alpha (1:1000, ab6671, Abcam), anti-MPO (1:1000, ab9535, Abcam), anti-Keap1 (1:1000, ab119403, Abcam), anti-p-Nrf2 (1:500, ab76026, Abcam), anti-Nrf2 (1:1000, ab137550, Abcam), and anti-HO-1 (1:2000, ab13248, Abcam). Band intensity was quantified using BandScan 5.0.

Statistical Analysis

Statistically significant differences were analyzed via Prism 7.0 and shown as the mean ± SD. ANOVA with Tukey's post hoc test and *t*-test were utilized to analyze the differences among multiple or two groups, respectively. Statistical significance was set at $p < 0.05$.

Results

Mst1 Was Downregulated in the Cardiac Tissue of MI Rats

To identify differentially expressed genes between the myocardial tissue of MI rats and healthy heart tissue, microarray analysis was performed on five MI hearts from the LAD-surgery animal model and five sham-control heart tissues. We found that Mst1 was in the top five downregulated genes (Fig. 1A). Next, we performed real-time PCR and WB to confirm its expression in the myocardial tissues. We observed that Mst1 in the cardiac tissue of MI rats was decreased at both the mRNA and protein levels (Fig. 1B, C), while the expression of other genes requires further validation (data not shown). Our data suggest that Mst1 expression is downregulated in the myocardial tissues of MI animals.

Furthermore, HBO preconditioning was used to alleviate cardiac damage caused by LAD surgery. It was clearly demonstrated that, compared with the non-administration group, Mst1 was upregulated in the myocardial tissue of MI rats in response to HBO administration (Fig. 1B, C). To investigate the role of Mst1 in HBO-alleviated cardiac function loss and injury in rats caused by MI modeling, LV-siMst1 was injected in situ into the heart tissue of MI rats to silence *Mst1* expression in HBO-preconditioned MI rats. Both real-time PCR and WB results showed that Mst1 expression was significantly decreased in MI rats, compared to that in the LV-siNC injection group (Fig. 1B, C).

HBO Preconditioning Relieves the Infarct Size and Pathological Alterations of MI Heart Tissue and Cardiac Function Loss, Whereas *Mst1* Silencing Abolished Its Effect

We performed TTC staining on the slices of heart samples from each group to assess the effect of Mst1 on infarct size in MI rats. TTC staining showed a significant improvement in infarct size reduction in the MI rat model in response to HBO administration (Fig. 2A, B). However, *Mst1* silencing reenlarged the infarct size in MI rats (Fig. 2A, B).

Blinded histological analysis of HE staining data showed that the HBO treatment group exhibited lower degrees of necrosis, neutrophilic infiltration, and hemorrhage than the

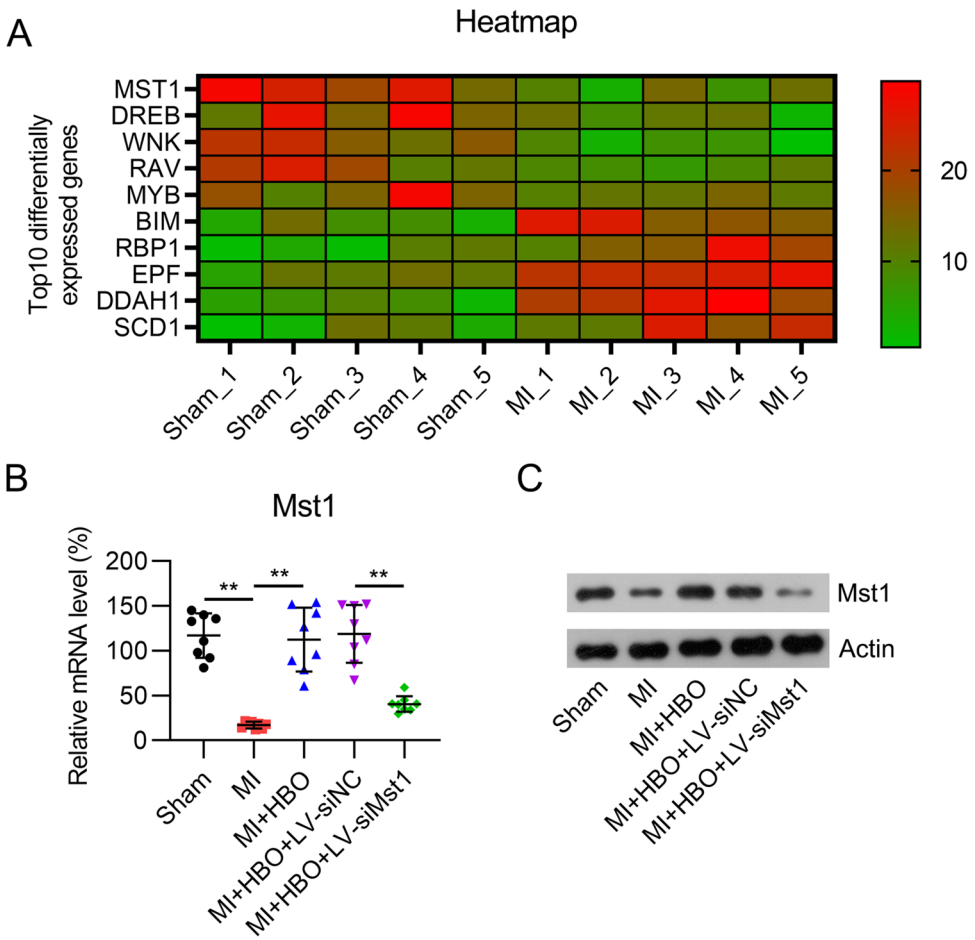

Fig. 1 Expression of Mst1 in cardiac tissue of MI rats with or without HBO preconditioning. **A** A microarray was performed to identify the differentially expressed genes between MI rat model and sham rats. The top five up- or downregulated genes in each cluster are displayed. Lentiviral infection was used to downregulate Mst1 expression in the myocardial tissue of MI rats with HBO preconditioning. **B** Real-time PCR and **C** WB analyses were performed to show the Mst1 expression in the cardiac tissue of rats with or without MI. $^{**}p < 0.01$

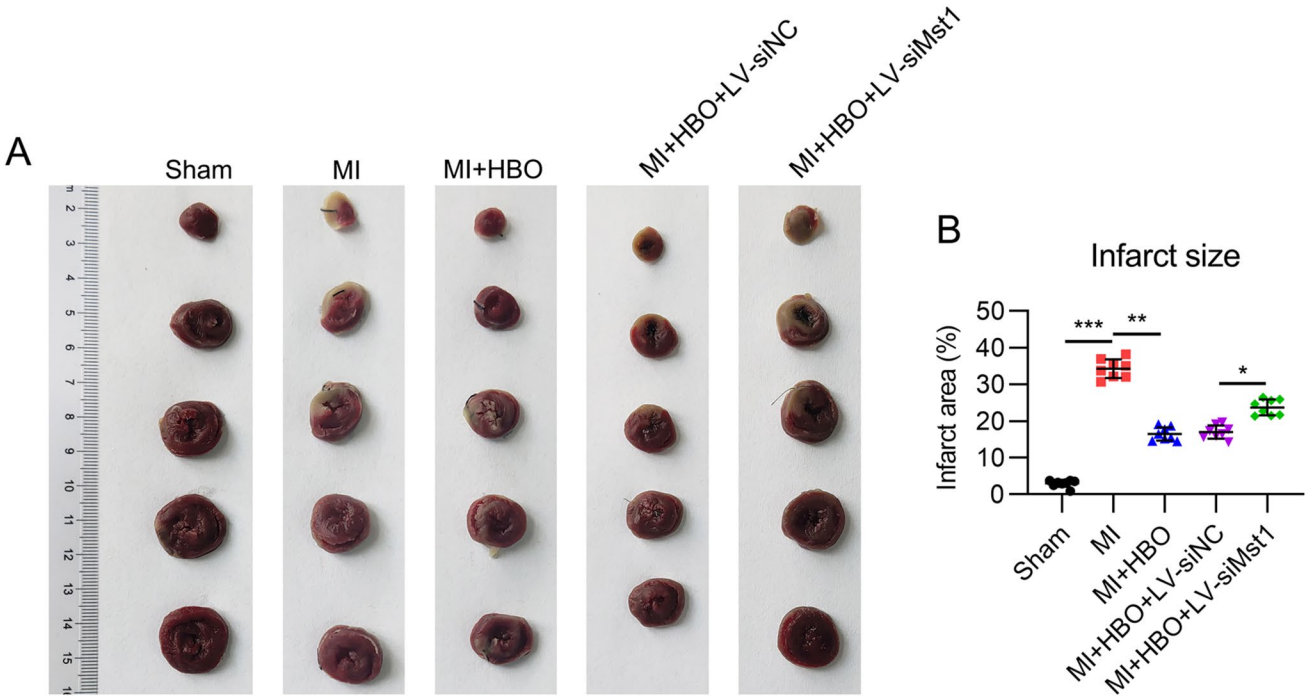

Fig. 2 Effects of HBO preconditioning and Mst1 silencing on MI-induced infarct in rats. **A** TTC staining was conducted to show the infarct size of the heart tissues of rats. **B** The right panel displays the infarct area of the heart tissue from the rats. $*p<0.05$, $**p<0.01$, $***p<0.001$

MI group. The LV-siNC-infected group showed no improvement in these abnormalities. However, in the LV-siMst1 group, histopathological changes in the myocardial tissue of MI rats were exacerbated even after HBO preconditioning (Fig. 3).

Electrocardiography was used to characterize the effect of HBO preconditioning and the involvement of Mst1 in the cardiac function loss caused by MI. Compared to the sham group, lower $\pm(dP/dt)$max and LVSP values and higher LVDP values, which indicated cardiac dysfunction, were observed in the MI group. As expected, HBO treatment resulted in alleviated cardiac dysfunction, as shown by recovered $\pm(dP/dt)$max, LVSP, and LVDP, compared with those in the MI group. After infection with LV-shMst1, the effects of HBO preconditioning on $\pm(dP/dt)$max, LVSP, and LVDP were reversed (Fig. 4A–C). Collectively, these data suggested that HBO preconditioning ameliorated MI-associated cardiac dysfunction in an Mst1-dependent manner.

Effect of HBO Preconditioning and Mst1 Involvement in Oxidative Disordering and Inflammation in the Myocardium Tissue of MI Rats

Oxidative disorders and inflammation are two features of MI development [20]. Therefore, we examined the effects of HBO preconditioning and Mst1 involvement on oxidative stress and inflammation in the myocardium of MI rats. The upregulation of myocardial MDA and 8-OHdG levels and downregulation of GSH activity demonstrated that MI caused significant oxidative stress in the myocardium. In the HBO preconditioning group, myocardial MDA and 8-OHdG

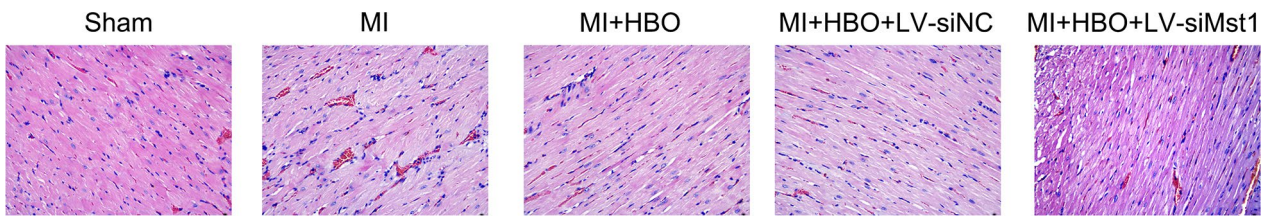

Fig. 3 Effect of HBO preconditioning and Mst1 silencing on pathophysiological events of MI mice. HE staining was used for histology analysis on myocardium tissue of rats

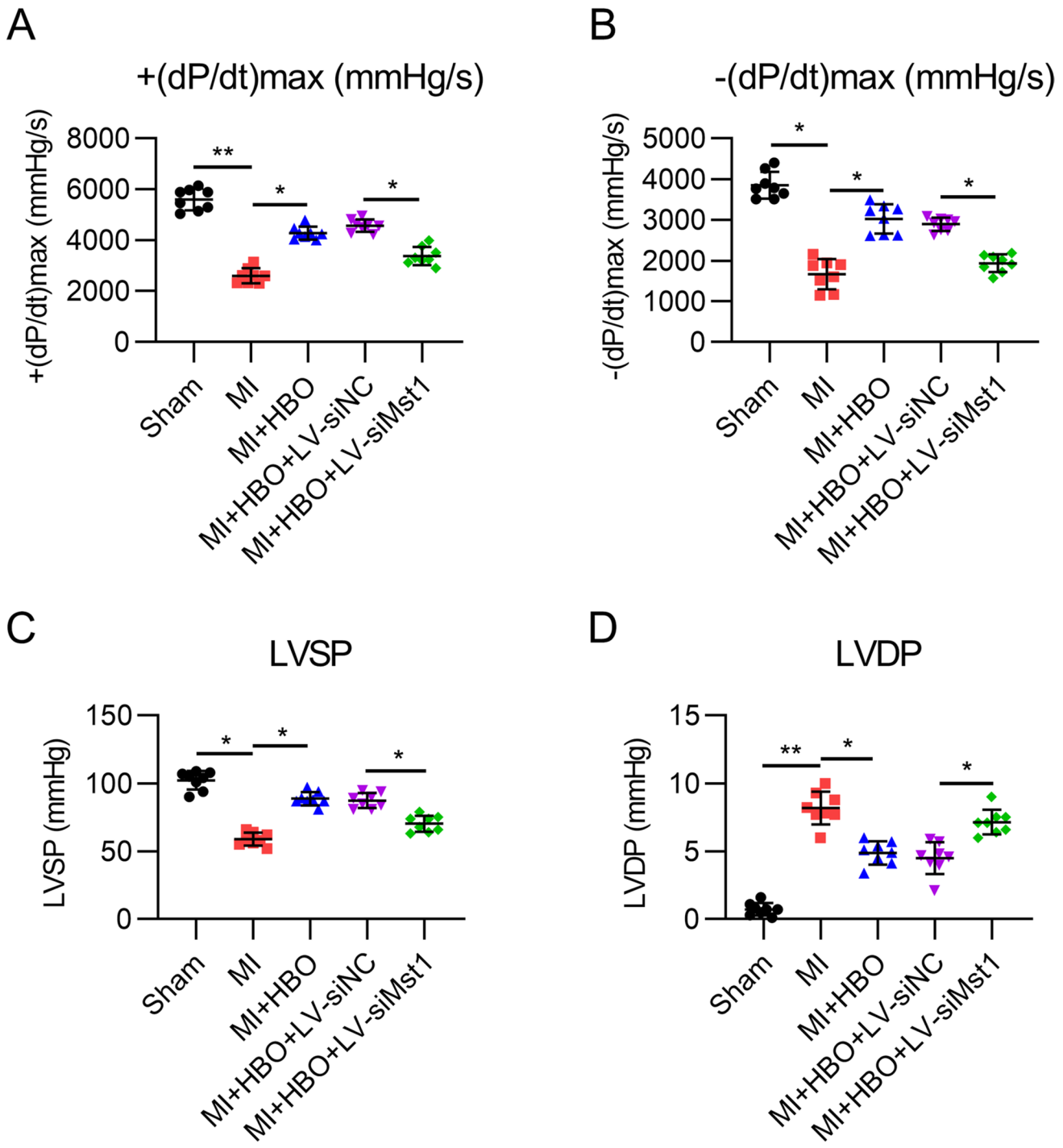

Fig. 4 Effect of HBO preconditioning and Mst1 silencing on the cardiac function of MI rats. The alterations in MI modeling-induced cardiac function were represented by **A**, **B** ±(d*P*/d*t*) max, **C** LVDP, and **D** LVSP, which were determined 24 days following LAD ligation surgery. $*p < 0.05$, $**p < 0.01$

levels were significantly reduced, whereas GSH activity was promoted in the myocardium. After infection with LV-siMst1, the alterations in myocardial MDA and 8-OHdG levels, as well as GSH activity in HBO-preconditioned MI rats, were recovered (Fig. 5A–C). These data demonstrate that HBO preconditioning alleviated oxidative stress in the myocardial tissue of MI rats via Mst1.

ELISA results indicated that inflammation-associated MPO and pro-inflammatory cytokines (IL-1β, and TNF-α) were robustly expressed in cardiac tissue in response

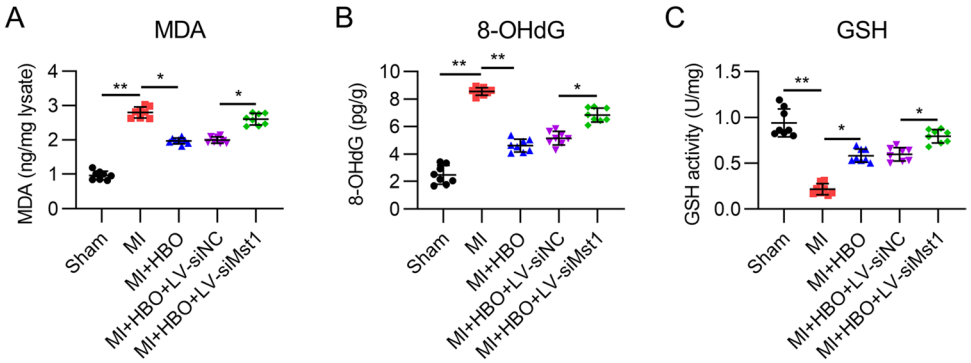

Fig. 5 Effect of HBO preconditioning and *Mst1* silencing on oxidative disordering in myocardium tissue of MI rats. Myocardium oxidative impairment was determined through **A** MDA, **B** 8-OHdG, and **C** GSH activity assays 24 days after LAD ligation surgery. *$p < 0.05$, **$p < 0.01$

to MI modeling, whereas HBO treatment alleviated the production of these cytokines (Fig. 6A–C). However, in HBO-preconditioned MI rats treated with LV-siMst1, the production of these three cytokines was significantly elevated. These data suggest that inflammation in MI heart tissue is inhibited by HBO treatment via Mst1 modulation.

Keap1/Nrf2/HO-1 Signaling Pathway in Myocardium of MI Rats Is Activated in Response to HBO Preconditioning

The Keap1/Nrf2/HO-1 signal transduction pathway is a well-documented pathway involved in cellular antioxidative functions [21], and a previous study demonstrated that Mst1

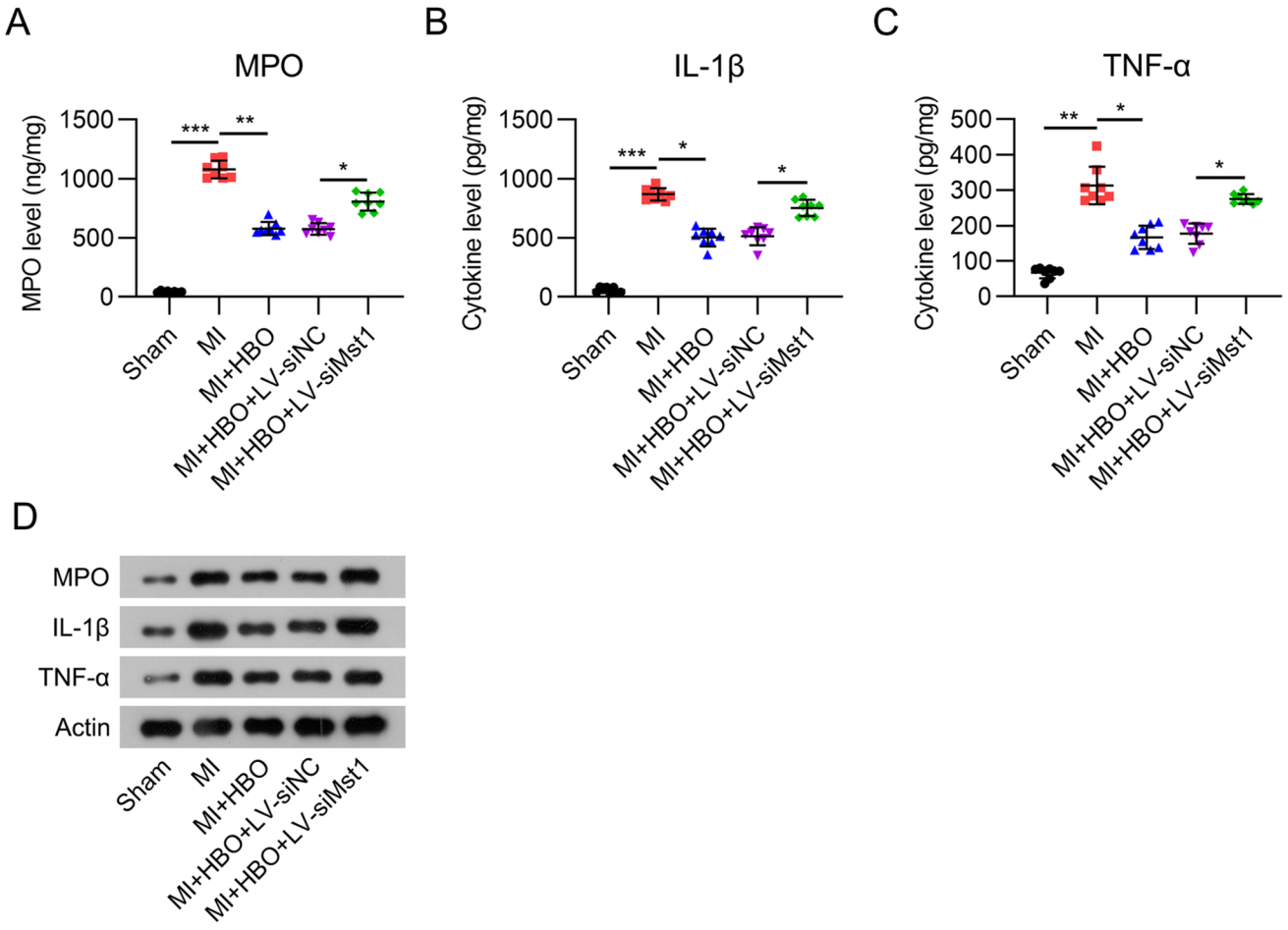

Fig. 6 Effect of HBO preconditioning and *Mst1* silencing on inflammation in myocardial tissue of MI rats. Inflammation in myocardium was evaluated via MPO, IL-1β, and TNF-α 24 days after LAD ligation surgery. *$p < 0.05$, **$p < 0.01$, ***$p < 0.001$

was able to activate this pathway by reducing Keap1 protein levels. Therefore, we hypothesized that HBO preconditioning could regulate oxidative stress via the potential regulatory role of Mst1 in the Keap1/Nrf2/HO-1 axis. WB results showed that Keap1 was induced, and that phosphorylated Nrf2, Nrf2, and HO-1 levels were decreased in the myocardium of MI rats, suggesting the deactivation of this pathway by MI modeling. In the HBO-treated group, we observed that Keap1 expression dramatically decreased, whereas Nrf2 and HO-1 expressions were elevated in myocardial tissue lysates. However, infection with LV-siMst1 restored Keap1 and reduced Nrf2 and HO-1 in HBO-exposed MI rats (Fig. 7), suggesting that the Keap1/Nrf2/HO-1 axis was activated by HBO preconditioning in an Mst1-dependent manner.

Discussion

In this study, using a rat model of acute MI, it was found that the expression of Mst1 decreased, whereas HBO preconditioning caused the upregulation of Mst1 in the myocardium tissue of MI rats. Also, our in vivo studies demonstrated that HBO reduced infarct size and alleviated histopathological changes and cardiac function loss in MI rats. Silencing *Mst1* expression in cardiac myocytes abolished the cardioprotective function of HBO preconditioning in MI rats. Furthermore, HBO preconditioning activated the Keap1/Nrf2/HO-1 axis in the myocardial tissue of MI rats in an MST-dependent manner. These results demonstrate that HBO alleviated MI-induced myocardial damage by upregulating the Mst1-modulated Keap1/Nrf2/HO-1 axis.

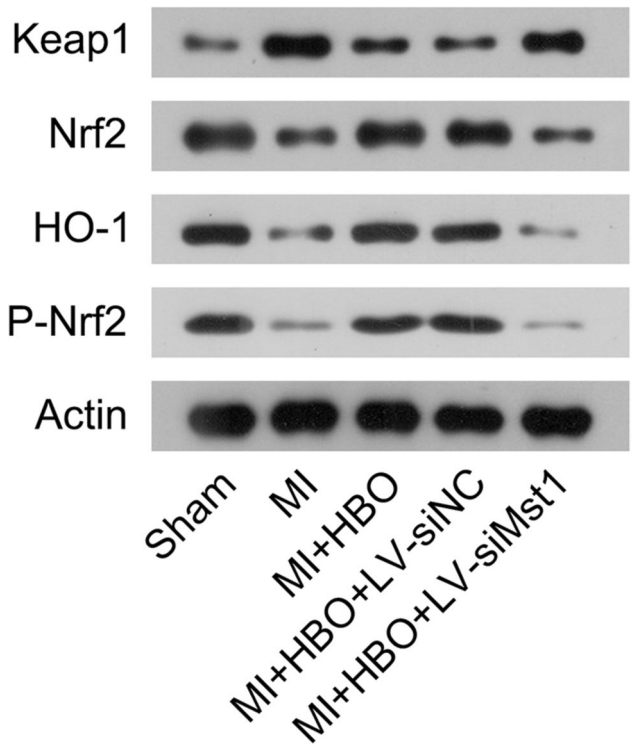

Fig. 7 Effect of HBO preconditioning and *Mst1* silencing on Keap1/Nrf2/HO-1 pathway activation in the myocardial tissue of MI rats. WB was utilized to determine the protein levels of Keap1, Nrf2, phosphorylated Nrf2, and HO-1 24 days after LAD ligation surgery

Previous studies have explored the effects of HBO preconditioning on MI development; however, their conclusions are unreliable. Radice et al. treated rats with 2.5 ATA HBO for 1 h, 3 h, or 6 h and subsequently removed the hearts and exposed them to low-flow ischemia and reperfusion [22]. Their findings showed that ischemia was aggravated in HBO-treated rats. Left ventricular end-diastolic pressure (LVEDP) was dramatically and proportionally elevated with HBO exposure time [22]. Maffei et al. exposed separate hearts to HBO and discovered that HBO markedly exacerbated postischemic impairment, as shown by elevated LVEDP and coronary perfusion pressure [23]. However, Han et al. indicated that HBO preconditioning could mitigate myocardial ischemia in a rat model [23]. The HBO-exposed group exhibited a smaller infarct size and markedly elevated LVSP, $-dP/dt$ max, and $+dP/dt$ max; VEGF protein levels and capillary density were also elevated [24]. Cabigas et al. reported that HBO preconditioning could reduce infarct size in separate hearts after IR, in which NOS plays a critical role [25]. A clinical study showed that HBO preconditioning before coronary artery bypass graft surgery resulted in an elevation in left ventricular stroke work 1 day after surgery and myocardial endothelial NOS and HSP72 levels, suggesting that HBO-PC was capable of providing endogenous cardioprotection after ischemia–reperfusion injury [26]. Yin et al. demonstrated that HBO preconditioning ameliorates myocardial IR injury by upregulating HO-1 expression [27]. The cause of the controversial results of HBO preconditioning is obscure and requires further clarification. In the present study, we used LAD ligation surgery to establish a MI rat model. Before MI modeling, four daily HBO pretreatments were administered. After MI modeling, the cardiac injury caused by MI was evidenced via infarct size determination, pathological changes, and cardiac function assessment. Our data clearly demonstrated that cardiac injury significantly improved after HBO preconditioning, which is consistent with several previous studies [23–27]. Our data also showed that HBO preconditioning resulted in HO-1 upregulation via Mst1 modulation, which is consistent with the findings of Yin et al. [27].

In addition to iron overload, the accumulation of oxidative stress is a major biochemical characteristic [28]. Morphological characteristics of robust oxidative disorders include mitochondrial shrinkage, mitochondrial cristae decrease or disappearance, elevated mitochondrial

membrane density and rupture, normal nuclear morphology, and lack of chromatin condensation [29]. This study showed that MDA and 8-OHdG levels were dramatically elevated, and that GSH in myocardial tissue with MI modeling was remarkably reduced. HBO treatment counteracted these alterations. These findings indicate that HBO preconditioning can alleviate oxidative disorders in the myocardial tissue of MI rats; however, the detailed effect of HBO on oxidative disordering-induced morphological features requires further clarification.

Our microarray results indicated the downregulation of Mst1 in the myocardial tissue of MI rats, which was confirmed through real-time PCR and WB. Mst1 is an oxidative stress regulator and is closely associated with mitochondrial function. As expected, increased Mst1 levels were detected in the myocardial tissue of MI rats in response to HBO preconditioning, suggesting an association between HBO and Mst1. Moreover, *Mst1* silencing abolished the cardioprotective role of HBO in MI rats by alleviating oxidative stress and inflammation. These data are consistent with those of a previous study demonstrating that the knockdown of *Mst1* in an MI cell model intensified cell injury via oxidative stress and inflammation. Therefore, it is reasonable to speculate that HBO functions in an Mst1-dependent manner. Excessive production of oxidants and cytokines exacerbates oxidative stress in mitochondria, leading to cell death [30, 31] and eventually causing myocardial injury.

Considering that Mst1 protein downregulation destroys the biological activities of antioxidant enzymes, an in-depth assay was conducted to clarify the mechanism underlying HBO-Mst1-mediating cell oxidative stress through Keap1/Nrf2/HO-1 pathway regulation. Nrf2 is capable of shielding cells from oxidative impairment by functioning as a critical transcription factor and oxidative stress sensor [12]. Deactivation of Keap1 can cause Nrf2 accumulation in the cell nucleus, accompanied by transcriptional activation of a series of genes that encode antioxidant and anti-inflammatory proteins, thereby reducing oxidative stress impairment. The protection part of Nrf2 and its target genes has been reported to ameliorate inflammatory responses and oxidative stress in myocardial IR injury [32]. Our data confirmed that HBO preconditioning resulted in the activation of this pathway, as indicated by upregulated phosphorylated Nrf2, Nrf2, and HO-1 levels. As expected, *Mst1* silencing counteracted the beneficial effect of HBO preconditioning on the antioxidative activity of Nrf2, suggesting that HBO preconditioning activates Nrf2 via Mst1 modulation.

Taken together, our results provide a novel mechanism for explaining the cardioprotective function of HBO preconditioning during MI development, which involves the activation of Mst1-dependent Keap1/Nrf2/HO-1 in the myocardium of MI animals. This study also confirmed that Mst1 assumes a critical role in cardioprotection, suggesting that Mst1 is a potential target for MI treatment in clinical therapy and drug development.

Author Contributions JL and YL designed the research plan. JL, YL, SW, ZZ, and DL performed the experiments and analyzed the data. DL wrote the manuscript.

Funding This research did not receive any specific grant from funding agencies in the public, commercial, or not-for-profit sectors.

Data Availability The data that support the findings of this study are available from the corresponding author [Di Li], upon reasonable request.

Declarations

Conflict of interest The authors declare that they have no conflict of interest.

Ethics Approval All procedures were approved by the Animal Care and Use Committee of Affiliated Hospital of Hebei Engineering University.

Consent to Participate Not applicable.

Consent to Publish Not applicable.

References

1. Wu, X., Reboll, M. R., Korf-Klingebiel, M., & Wollert, K. C. (2021). Angiogenesis after acute myocardial infarction. *Cardiovascular Research, 117*, 1257–1273.
2. Tuk, B., Tong, M., Fijneman, E. M., & van Neck, J. W. (2014). Hyperbaric oxygen therapy to treat diabetes impaired wound healing in rats. *PLoS ONE, 9*, e108533.
3. Kimmel, H. M., Grant, A., & Ditata, J. (2016). The presence of oxygen in wound healing. *Wounds, 28*, 264–270.
4. Yümün, G., Kahraman, C., Kahraman, N., Yalçınkaya, U., Akçılar, A., Akgül, E., & Vural, A. H. (2016). Effects of hyperbaric oxygen therapy combined with platelet-rich plasma on diabetic wounds: An experimental rat model. *Archives of Medical Science, 12*, 1370–1376.
5. Sun, Q., Sun, Q., Liu, Y., Sun, X., & Tao, H. (2011). Anti-apoptotic effect of hyperbaric oxygen preconditioning on a rat model of myocardial infarction. *Journal of Surgical Research, 171*, 41–46.
6. Dotsenko, E., Nikulina, N., Salivonchik, D., Lappo, O., Gritsuk, A., & Bastron, A. (2015). Low doses of hyperbaric oxygenation effectively decrease the size of necrotic zone in rats with experimental myocardial infarction. *Bulletin of Experimental Biology and Medicine, 158*, 732–734.
7. Bennett, M. H., Lehm, J. P., & Jepson, N. (2015). Hyperbaric oxygen therapy for acute coronary syndrome. *Cochrane Database of Systematic Reviews, 2015*(7), 4818.
8. Chen, C., Huang, L., Nong, Z., Li, Y., Chen, W., Huang, J., Pan, X., Wu, G., & Lin, Y. (2017). Hyperbaric oxygen prevents cognitive impairments in mice induced by D-galactose by improving cholinergic and anti-apoptotic functions. *Neurochemical Research, 42*, 1240–1253.
9. Chen, X., Li, Y., Chen, W., Nong, Z., Huang, J., & Chen, C. (2016). Protective effect of hyperbaric oxygen on cognitive impairment induced by D-galactose in mice. *Neurochemical Research, 41*, 3032–3041.

10. Yang, J., Chen, W., Zhou, X., Li, Y., Nong, Z., Zhou, L., Wei, X., Pan, X., Chen, C., & Lu, W. (2022). Hyperbaric oxygen protects against PC12 and H9C2 cell damage caused by oxygen–glucose deprivation/reperfusion via the inhibition of cell apoptosis and autophagy. *Biocell, 46*, 137.
11. Yu, W., Xu, M., Zhang, T., Zhang, Q., & Zou, C. (2019). Mst1 promotes cardiac ischemia–reperfusion injury by inhibiting the ERK-CREB pathway and repressing FUNDC1-mediated mitophagy. *The Journal of Physiological Sciences, 69*, 113–127.
12. McClatchey, A. I., & Giovannini, M. (2005). Membrane organization and tumorigenesis—The NF2 tumor suppressor, Merlin. *Genes and Development, 19*, 2265–2277.
13. Rothzerg, E., Ingley, E., Mullin, B., Xue, W., Wood, D., & Xu, J. (2021). The Hippo in the room: Targeting the Hippo signalling pathway for osteosarcoma therapies. *Journal of Cellular Physiology, 236*, 1606–1615.
14. Hui, Q., Karlstetter, M., Xu, Z., Yang, J., Zhou, L., Eilken, H. M., Terjung, C., Cho, H., Gong, J., & Lai, M. J. (2020). Inhibition of the Keap1-Nrf2 protein–protein interaction protects retinal cells and ameliorates retinal ischemia–reperfusion injury. *Free Radical Biology and Medicine, 146*, 181–188.
15. Xu, B., Zhang, J., Strom, J., Lee, S., & Chen, Q. M. (2014). Myocardial ischemic reperfusion induces de novo Nrf2 protein translation. *Biochimica et Biophysica Acta (BBA) Molecular Basis of Disease, 1842*, 1638–1647.
16. Shyu, K.-G., Lu, M.-J., Chang, H., Sun, H.-Y., Wang, B.-W., & Kuan, P. (2005). Carvedilol modulates the expression of hypoxia-inducible factor-1α and vascular endothelial growth factor in a rat model of volume-overload heart failure. *Journal of Cardiac Failure, 11*, 152–159.
17. Bouachour, G., Cronier, P., Gouello, J. P., Toulemonde, J. L., Talha, A., & Alquier, P. (1996). Hyperbaric oxygen therapy in the management of crush injuries: A randomized double-blind placebo-controlled clinical trial. *Journal of Trauma, 41*, 333–339.
18. Gao, S., Li, G., Shao, Y., Wei, Z., Huang, S., Qi, F., Jiao, Y., Li, Y., Zhang, C., & Du, J. (2021). FABP5 deficiency impairs mitochondrial function and aggravates pathological cardiac remodeling and dysfunction. *Cardiovascular Toxicology, 21*, 619–629.
19. Livak, K. J., & Schmittgen, T. D. (2001). Analysis of relative gene expression data using real-time quantitative PCR and the 2(−Delta Delta C(T)) method. *Methods, 25*, 402–408.
20. Neri, M., Fineschi, V., Di Paolo, M., Pomara, C., Riezzo, I., Turillazzi, E., & Cerretani, D. (2015). Cardiac oxidative stress and inflammatory cytokines response after myocardial infarction. *Current Vascular Pharmacology, 13*, 26–36.
21. Baird, L., & Yamamoto, M. (2020). The molecular mechanisms regulating the KEAP1-NRF2 pathway. *Mol Cell Biol, 40*(13), e00099-20.
22. Radice, S., Rossoni, G., Oriani, G., Michael, M., Chiesara, E., & Berti, F. (1997). Hyperbaric oxygen worsens myocardial low flow ischemia–reperfusion injury in isolated rat heart. *European Journal of Pharmacology, 320*, 43–49.
23. Maffei Facino, R., Carini, M., Aldini, G., Berti, F., & Rossoni, G. (1999). *Panax ginseng* administration in the rat prevents myocardial ischemia–reperfusion damage induced by hyperbaric oxygen: Evidence for an antioxidant intervention. *Planta Medica, 65*, 614–619.
24. Han, C., Lin, L., Zhang, W., Zhang, L., Lv, S., Sun, Q., Tao, H., Zhang, J. H., & Sun, X. (2008). Hyperbaric oxygen preconditioning alleviates myocardial ischemic injury in rats. *Experimental Biology and Medicine (Maywood, N.J.), 233*, 1448–1453.
25. Cabigas, B. P., Su, J., Hutchins, W., Shi, Y., Schaefer, R. B., Recinos, R. F., Nilakantan, V., Kindwall, E., Niezgoda, J. A., & Baker, J. E. (2006). Hyperoxic and hyperbaric-induced cardioprotection: Role of nitric oxide synthase 3. *Cardiovascular Research, 72*, 143–151.
26. Jeysen, Z. Y., Gerard, L., Levant, G., Cowen, M., Cale, A., & Griffin, S. (2011). Research report: The effects of hyperbaric oxygen preconditioning on myocardial biomarkers of cardioprotection in patients having coronary artery bypass graft surgery. *Undersea and Hyperbaric Medicine, 38*, 175–185.
27. Yin, X., Wang, X., Fan, Z., Peng, C., Ren, Z., Huang, L., Liu, Z., & Zhao, K. (2015). Hyperbaric oxygen preconditioning attenuates myocardium ischemia–reperfusion injury through upregulation of heme oxygenase 1 expression: PI3K/Akt/Nrf2 pathway involved. *Journal of Cardiovascular Pharmacology and Therapeutics, 20*, 428–438.
28. Latunde-Dada, G. O. (2017). Ferroptosis: Role of lipid peroxidation, iron and ferritinophagy. *Biochimica et Biophysica Acta General Subjects, 1861*, 1893–1900.
29. Souza-Neto, F. V., Islas, F., Jiménez-González, S., Luaces, M., Ramchandani, B., Romero-Miranda, A., Delgado-Valero, B., Roldan-Molina, E., Saiz-Pardo, M., Cerón-Nieto, M., Ortega-Medina, L., Martínez-Martínez, E., & Cachofeiro, V. (2022). Mitochondrial oxidative stress promotes cardiac remodeling in myocardial infarction through the activation of endoplasmic reticulum stress. *Antioxidants (Basel), 11*, 1232.
30. Brazão, V., Colato, R. P., Santello, F. H., Vale, GTd., Gonzaga, Nd. A., Tirapelli, C. R., & Prado Jr, JCd. (2018). Effects of melatonin on thymic and oxidative stress dysfunctions during *Trypanosoma cruzi* infection. *Journal of Pineal Research, 65*, e12510.
31. Ding, M., Ning, J., Feng, N., Li, Z., Liu, Z., Wang, Y., Wang, Y., Li, X., Huo, C., & Jia, X. (2018). Dynamin-related protein 1-mediated mitochondrial fission contributes to post-traumatic cardiac dysfunction in rats and the protective effect of melatonin. *Journal of Pineal Research, 64*, e12447.
32. Yao, H., He, Q., Huang, C., Wei, S., Gong, Y., Li, X., Liu, W., Xu, Z., Wu, H., & Zheng, C. (2022). Panaxatriol saponin ameliorates myocardial infarction-induced cardiac fibrosis by targeting Keap1/Nrf2 to regulate oxidative stress and inhibit cardiac-fibroblast activation and proliferation. *Free Radical Biology and Medicine, 190*, 264–275.